# Technical Note on CaNoE Entry for MLDC Round 3.4

Ilya Mandel*
*Department of Physics and Astronomy, Northwestern University, 2131 Tech Dr., Evanston, IL 60208*

Jonathan R Gair†
*Institute of Astronomy, Madingley Road, CB3 0HA, Cambridge, UK*
(Dated: May 1, 2009)

We carried out an analysis of Mock LISA Data Challenge 3.4 using time-frequency techniques. We used a modification of the Chirp-based Algorithm for Track Search (CATS) to locate vertical tracks characterized by time, starting frequency, and ending frequency on a spectrogram of the data [1, 2]. We were able to identify three burst sources in Challenge 3.4 data. We estimated their central time at the detector and the $f_{\max}$ frequency.

## I. TRACK DETECTION: CATS

We used an improved version of the Chirp-based Algorithm for Track Search [1, 2] to find tracks on a time-frequency spectrogram. CATS is essentially a grid-based search on a spectrogram for tracks of a given shape. For the this challenge, we parametrized vertical tracks by three parameters: time bin and the starting and ending frequency bins.

In general, a CATS search proceeds as follows:

- Construct $A$ and $E$ channels from the bandpassed challenge data stream (we used Synthetic LISA data).
- For each channel, construct a spectrogram by dividing the data into overlapping time segments of equal duration, then Fourier transforming the data in each time segment after multiplying it by a Hanning window to reduce edge effects.
- Normalize the two spectrograms by dividing the signal power in each pixel by the expected LISA noise power spectral density, then construct a joint spectrogram by adding the two normalized spectrograms.
- Construct a grid of parameters; for each point in the parameter space, build a potential track and determine the power in the pixels along this track.
- Compute the CATS track power statistic which is chosen to optimize track detection for a given false alarm probability. Keep a list of all tracks that exceed a power statistic chosen to yield only tracks exceeding a fixed false alarm probability.
- Sort all found tracks by the CATS power statistic.
- Go down the list of sorted tracks and retain only those tracks which do not share any pixels with the tracks above them; thus, construct a sorted list of non-overlapping tracks whose power statistic exceeds a threshold.

Figure 1 shows a spectrogram of a portion of the Challenge 3.4 data, overplotted with tracks detected by CATS. (We cut off the search for tracks at a frequency of 0.027 Hz because of the presence of several bright noise lines at higher frequencies.)

A number of parameters in the above procedure can be varied. These include the starting and ending time of the search, the lower and upper frequencies of the search window, and the duration of time bins used to create the spectrogram. For vertical burst tracks, wider bins yield better frequency resolution, while narrow bins allow for a more precise measurement of the burst's central time.

---

*Electronic address: `ilyamandel@chgk.info`
†Electronic address: `jgair@ast.cam.ac.uk`

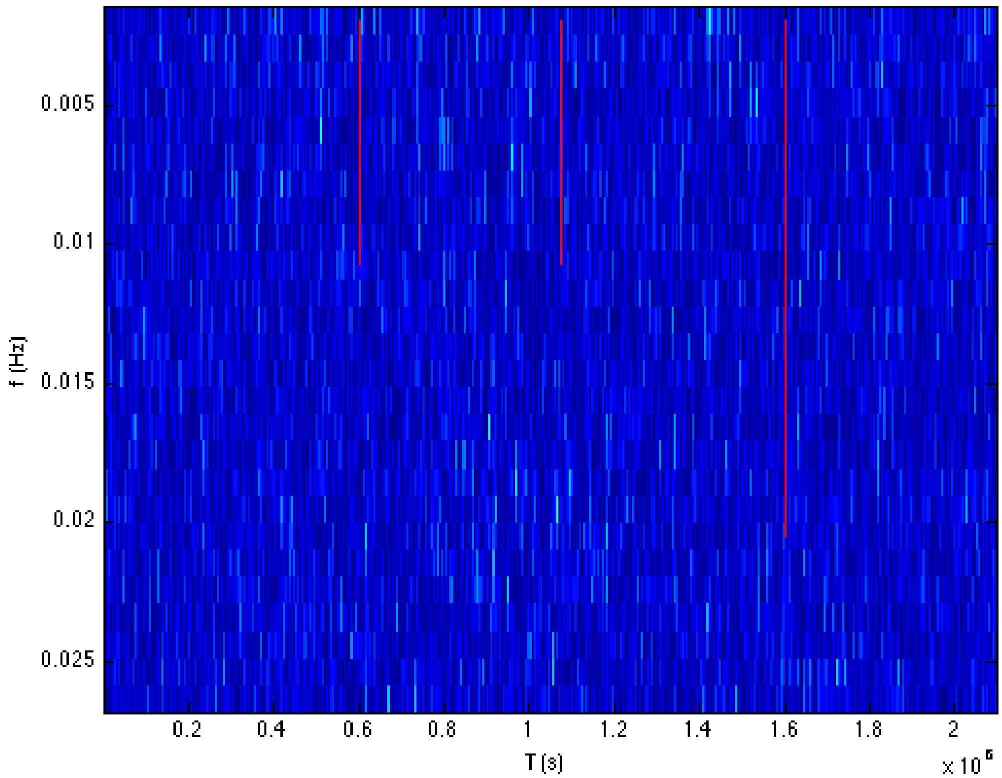


FIG. 1: A spectrogram of a portion of the data from C3.4 with the vertical tracks detected by CATS plotted over in red.

| Track Number | Central Time (s) | $f_{\max}$ |
|---|---|---|
| 1 | 599695 | undetermined (0.5 Hz) |
| 2 | 1073140 | 0.0013 Hz |
| 3 | 1602610 | undetermined (0.5 Hz) |

TABLE I: Challenge 3.4: Estimates of parameters resolvable with a time-frequency search

## II. SEARCH RESULTS AND PARAMETER ESTIMATION

We were able to detect three burst tracks in Challenge 3.4 data. We estimated their central times and the values of $f_{\max}$ as shown in Table II. We did not estimate the sky location, polarization, or the source amplitude.

We were able to find the central time of the source by picking sufficiently narrow time bins. (Note, however, that this is the time of the burst arrival at the detector, not in the solar-system barycenter — we could not determine the latter since we did not estimate the sky location of the source.) For sources 1 and 3, the timing error is probably on the order of 10–20 seconds, since we were able to decrease the time bins down to 32 seconds. However, for source 2, which was only significant at low frequencies, such narrow time bins could not be used, and the timing error could be $\sim 50$ seconds.

We found that although the normalized power in the $A$ and $E$ channels depended significantly on all of the source parameters, the variation of the sum of the power $A+E$ with frequency primarily depended only on the value of $f_{\max}$. The solid curves in Figure 2 shows the variation of the power $A+E$ as a function of frequency for different values of $f_{\max}$ with all other parameters fixed. We plotted the measured variation for the three sources 1, 2, and 3 with dashed lines. The variation for sources 1 (red) and 3 (blue) was consistent with the highest value of $f_{\max}$ that we were sensitive to; we therefore reported these sources as having $f_{\max} = 0.5$Hz, though we are not sensitive beyond about

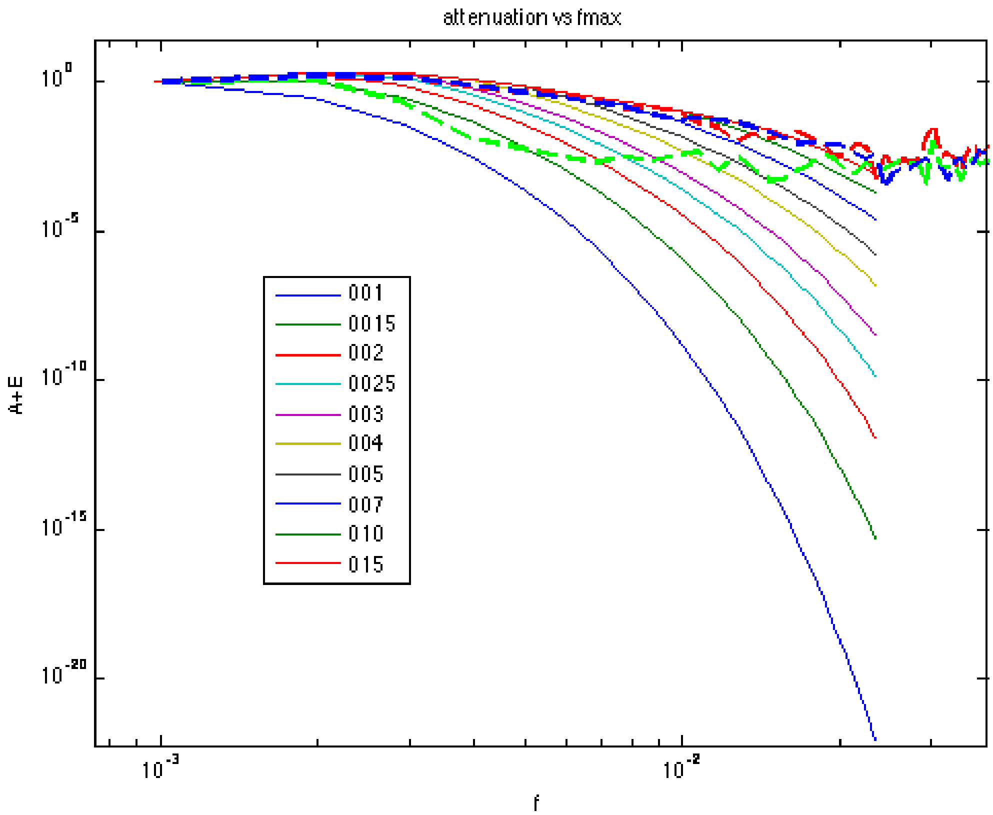


FIG. 2: The variation of the sum of the normalized power in the $A$ and $E$ channels with frequency for different values of $f_{\max}$ (solid curves). The dashed curves show the measured variation for sources 1 (red), 2 (green), and 3 (blue).

15 mHz. Source 2 (green) showed clear attenuation at low frequency, though it deviated from predicted behavior at higher frequencies due to limited SNR. Because the attenuation of power with frequency at low frequencies placed this source between the curves corresponding to $f_{\max} = 0.001$Hz and $f_{\max} = 0.0015$Hz, we estimated the cutoff frequency for this curve as $f_{\max} = 0.0013$Hz.

[1] Gair JR, Mandel I and Wen L, CQG 25, 184031; arXiv:0804.1084
[2] Mandel I and Gair J R, in preparation